

# Exact Limits of Inference in Coalescent Models

James E. Johndrow and Julia Palacios

*390 Serra Mall  
Stanford, California, 94305*

*e-mail: [johndrow@stanford.edu](mailto:johndrow@stanford.edu), [juliapr@stanford.edu](mailto:juliapr@stanford.edu)*

**Abstract:** Recovery of population size history from sequence data and testing of hypotheses about features of population size history are important problems in population genetics. Inference commonly relies on a coalescent-based model linking the population size history to genealogies. We consider the problem of recovering the true population size history from two possible alternatives on the basis of coalescent time data. We give exact expressions for the probability of selecting the correct alternative in a variety of biologically interesting cases as a function of the separation between the alternative size histories, the number of genealogies and loci sampled, and the sampling times. The results are applied to human population history. As coalescent times are inferred from sequence data rather than directly observed, the inferential limits we give can be viewed as optimistic.

## 1. Introduction

Estimation of effective past population size trajectories from genetic data provides insight into how genetic diversity evolves over time. Availability of molecular sequence data from different organisms living today and from ancient DNA samples has enabled reconstruction of effective population size trajectories of human populations over the past 300,000 years [6, 12], Ebola virus over the 2014 epidemic in Sierra Leone [18] and Egyptian hepatitis C virus for over 100 years [8].

Until recently, inferences of effective population size trajectories was limited by scarce availability of molecular sequence data such as single nucleotide polymorphisms (SNPs) and microsatellites. The ongoing large-scale increase in the total amount of genetic data obtained at different time points from large number of individuals over large genomic segments (loci) has led to a situation in which computationally tractable statistical inference is only available from non-sufficient summary statistics such as the site frequency spectra (SFS) [14] or from small numbers of samples [11].

Many statistical inference methods that have been proposed over the last 15 years have been applied to inference of human population history. Several studies agree that non-African populations have experienced two severe bottlenecks, one attributed to the expansion Out-of-Africa and the other attributed to the separation of Asian and European populations. There is however, disagreement

in the timing and length of such events. Although statistical power is affected by the data generation process such as genotyping quality and the sample selection process, it is natural to wonder how increasing the amount of genetic data increases our ability to distinguish between alternative hypotheses about population history.

The standard  $n$ -coalescent [10] is a generative model of molecular sequence of  $n$  individuals sampled at random from a population of interest. In the single-locus neutral model, observed variation is the result of a stochastic process of mutations along the branches of the sample's genealogy; the genealogy is a timed bifurcating tree that represents the ancestral relationships among samples. When moving back in time, two individuals find a common ancestor (coalesce) in the past with rate inversely proportional to the effective population size  $N(t)$ . Initially, the standard (homogeneous)  $n$ -coalescent assumed constant population size  $N(t) = N$  and that sequences were sampled at the same time ( $t=0$ ); assuming a global mutation rate  $\mu$ , the parameter of interest is  $\theta = 2N\mu$ . The standard neutral coalescent has been extended to variable population size  $N(t)$  [15], varying sampling times (heterochronous coalescent [3]), and to account for population structure [1] and recombination [7].

In the constant population model ( $\theta = 2N\mu$ ), different authors [4, 13, 2] argued that accuracy of estimators of  $\theta$ , measured in terms of the squared coefficient of variation, increases linearly in the number of independent loci and logarithmically in the number of samples, and it is not affected by the sequence length. In addition, Pluzhnikov and Donnelly [13] considered the constant population model with recombination and argued that when the recombination rate is high, increasing the sequence length effectively increases the number of independent loci. Indeed, when two genomic segments are separated by a recombination event, these two segments (loci) derive from two different but correlated genealogies. As the number of recombination events increases, the correlation between the two genealogies becomes weaker, and hence increasing the length of sequenced segments increases the opportunity to observe a larger number of realizations from independent (unlinked) loci [12, 7].

In the coalescent model with variable population size, Terhorst and Song [17] showed that estimators of  $N(t)$  based on the SFS have an extremely slow minimax rate of convergence. The authors argue that the minimax rate of convergence is inversely proportional to the logarithm of the number of independent loci and does not depend at all on the number of individuals sampled. Kim et al. [9] provided bounds on the Bayes error rate achievable to distinguish between two population histories in the idealized setting of observing the genealogy of the sample. The authors show that Bayes error rate decreases proportionally to the number of loci but do not explore the effect of larger samples and recombination. Moreover, as we show here, in some cases their bounds are not tight enough to drive insight about the amount information needed.

The neutral coalescent with variable population size is a point process of coalescent events whose rate depends on  $N(t)$ . For a sample of size  $n$ , the  $n - 1$  coalescent times are sufficient statistics for inferring  $N(t)$ . Unfortunately, the  $n - 1$  coalescent times are hardly ever observable. Instead we observe molecular

variation that reflects a process of mutation superimposed to the genealogical process. Several estimators exist from different summary statistics. Gao and Keinan [5] show an extensive list of several methods.

Instead of assessing the performance of specific estimators, we give a series of results on the probability that any procedure can identify the true population size history from a set of two alternatives on the basis of directly observed coalescent time data. All of our results are exact. We begin with the case of a single locus and single observed coalescent time and gradually build up to more complicated settings with more than one locus or multiple observed coalescent times. We also give some consideration to sampling times and recombination. We improve upon previously estimated upper bounds [9], and show that in many cases the previous bounds are quite loose. We further confirm previous assessments in the constant population setting about diminishing returns to more samples and linearly increasing returns to more independent loci. In an example motivated by the Out of Africa human bottleneck, we quantify exactly the limits of inference for any procedure as a function of the number of loci and sampling times, suggesting that the inferential problem is quite difficult using only samples from the present-day population.

## 2. Background and Preliminaries

We consider the  $n$ -coalescent model of a genealogy of  $n$  individuals in the case where  $n - 1$  coalescent times are observed. Let  $x_n = 0$  denote the present time and let  $x_n = 0 < x_{n-1} < \dots < x_1$  denote the coalescent times of lineages in the genealogy with time running backward. The coalescent process is a Markov point process, and the likelihood of coalescent time  $x_{k-1}$  is defined conditionally as

$$L(x_k | x_{k-1}, N_e(t)) = \frac{C_k}{N_e(x_{k-1})} \exp \left\{ - \int_{x_k}^{x_{k-1}} \frac{C_k}{N_e(t)} dt \right\}$$

where  $C_k = \binom{k}{2}$  is the combinatorial factor depending on the number of possible ways that two lineages can coalesce given that there are  $k$  lineages, and  $N_e(t)$  is the *effective population size*, a function of time. It follows that the complete likelihood is given by

$$\begin{aligned} L(x_1, \dots, x_n | N_e(t)) &= p(x_n) \prod_{k=n}^2 p(x_{k-1} | x_k, N_e(t)) \\ &= \prod_{k=n}^2 \frac{C_k}{N_e(x_{k-1})} \exp \left\{ - \int_{x_k}^{x_{k-1}} \frac{C_k}{N_e(t)} dt \right\} \end{aligned} \quad (2.1)$$

where again  $x_n \equiv 0$  by definition.

Motivated in part by [9], we consider simple hypothesis tests of the form

$$H_1 : N_e(t) = aN_0, \quad T \leq t \leq T + S$$

$$H_2 : N_e(t) = bN_0, \quad T \leq t \leq T + S$$

with  $N_e(t)$  equal under  $H_1$  and  $H_2$  outside the interval  $[T, T + S]$ . Note that  $T = 0, S = \infty$  is also considered. Kim et al. [9] show upper bounds on the probability of correctly identifying  $H_1$  or  $H_2$  in the case where  $J$  independent pairwise coalescence times are observed. This arises when we have  $J$  samples each consisting of two individuals (equivalently, one coalescence time) and the samples are independent, as would occur when the genealogies are inferred from independently segregating loci. Here we obtain exact expressions rather than upper bounds, and extend results to the case where our data consist of  $n$  individuals ( $n - 1$  coalescence times). We derive analytic expressions for arbitrary  $n$  when  $N_2(t) = cN_1(t)$  for all  $t$ , and obtain bounds for  $n = 3$  in more general settings. Comparison of our exact calculations to the Hellinger bounds from [9] show that in some cases the bounds are quite loose.

We now give some additional background and then review some of the results in [9]. We will work in the simple hypothesis testing setting in which there are two hypotheses under consideration,  $H_1$  and  $H_2$ , and our goal is to determine which hypothesis represents the true state of nature under which the data were generated. For simplicity of notation, we associate the state of nature with a parameter  $\vartheta \in \{1, 2\}$  such that  $H_1 : \vartheta = 1$  and  $H_2 : \vartheta = 2$ . Recall that a (binary) Bayes classifier or decision rule  $\vartheta(x)$  has the form

$$\vartheta(x) = \mathbf{1}_{\{\text{BF}_{12}(x) < 1\}} + 1,$$

where  $\text{BF}_{12}(x)$  is the Bayes factor for  $H_1$  vs  $H_2$ ,  $\mathbf{1}_A$  is the indicator of the event  $A$ , and  $x$  is an observation of a random variable  $X$  with likelihood  $L(x \mid \theta)$ . In the sequel, we drop the explicit argument and simply write  $\text{BF}_{12}$  in place of  $\text{BF}_{12}(x)$ . Thus, if  $\vartheta(x)$  returns 1, we infer that the data were generated under  $H_1$ , whereas if  $\vartheta(x)$  returns 2, we infer that the data were generated under  $H_2$ . Kim et al. [9] prove results for Bayes classifiers in the case where each hypothesis is assigned prior probability of one half. In this case, the Bayes classifier reduces to the maximum likelihood estimate of the unknown state of nature  $H_j$ ,  $j = 1, 2$ . When the prior is correct, the Bayes classifier is the optimal classifier, so that the probability of correct classification using the Bayes classifier is the maximum achievable probability. As such, by studying the properties of the Bayes classifier, we obtain general limitations on inference for any classifier or test.

We first define some notation. Let  $X = (X_1, X_2, \dots, X_{n-1})$  be the random vector of coalescent times with distribution given by (2.1) under  $H_1$  and  $Y = (Y_1, Y_2, \dots, Y_{n-1})$  be the random vector of coalescent times with distribution given by (2.1) under  $H_2$ . Further, when multiple genealogies are available, we will denote the random vector of coalescent times corresponding to the  $j$ -th genealogy by  $X^j$ .

The strategy for proving bounds in Kim et al. [9] is the following. Consider the likelihood in (2.1) with  $n = 2$ , and suppose  $J$  independent observations are generated by the prior, so that with probability  $1/2$  either  $H_1$  or  $H_2$  is selected and then  $J$  iid pairwise coalescence times are generated under that hypothesis.

In this case, the Bayes error rate for any classifier is at least  $(1 - \Upsilon)/2$  where

$$\Upsilon = \mathbf{P}[\vartheta(x) = \vartheta] - \mathbf{P}[\vartheta(x) \neq \vartheta] = d_{\text{TV}}(X^J, Y^J),$$

and where for two probability measures  $\mu, \nu$  and corresponding random variables  $X \sim \mu, Y \sim \nu$ ,

$$\begin{aligned} d_{\text{TV}}(X, Y) &= d_{\text{TV}}(\mu, \nu) \equiv \sup_A |\mu(A) - \nu(A)| = \inf_{\Gamma \in \mathcal{C}(\mu, \nu)} \int \mathbf{1}\{x \neq y\} \Gamma(dx, dy) \\ &= \sup_{|f| < 1} \frac{1}{2} \int f(x)(\mu - \nu)(dx), \end{aligned}$$

is the total variation distance between probability measures  $\mu, \nu$ , and  $\mathcal{C}(\mu, \nu)$  is the space of all couplings of  $\mu, \nu$ . They then apply Kraft's inequality [16, equation 5.7],

$$\frac{1}{2} d_{\text{TV}}^2 \leq d_{\text{H}}^2$$

where  $d_{\text{H}}$  is the *Hellinger distance*. Let  $P$  and  $Q$  be probability measures that are absolutely continuous with respect to some dominating measure  $\lambda$ , and let  $f_P = \frac{dP}{d\lambda}$ ,  $f_Q = \frac{dQ}{d\lambda}$  be their respective Radon-Nikodym derivatives. The Hellinger distance between  $P$  and  $Q$  is defined by

$$d_{\text{H}}^2(P, Q) = \frac{1}{2} \int (\sqrt{f_P} - \sqrt{f_Q})^2 d\lambda.$$

In the case where  $\lambda$  is Lebesgue measure,  $f_P$  and  $f_Q$  are the densities of  $P$  and  $Q$ . The main result of [9] is

**Theorem 2.1** (Kim et al. [9], Theorem 1). *Suppose  $n = 2$  in (2.1). Then*

$$d_{\text{H}}^2(X^1, Y^1) = e^{-\int_0^T \frac{1}{N_e(t)} dt} \left( 1 - e^{-\frac{(a+b)S}{2abN_0}} \right) \frac{(\sqrt{a} - \sqrt{b})^2}{a + b}.$$

We give a proof in the appendix that fills in some additional details of the proof in [9]. Rather than obtaining bounds on the Bayes error rate using the Hellinger distance, we compute the probability of correct inference on  $\vartheta$  by

$$\begin{aligned} \mathbf{P}[\vartheta(x) = \vartheta] &= \mathbf{P}[\vartheta(x) = 1 \mid H_1] \mathbf{P}[H_1] + \mathbf{P}[\vartheta(x) = 2 \mid H_2] \mathbf{P}[H_2] \\ &= \mathbf{P}[\text{BF}_{12} > 1 \mid H_1] \mathbf{P}[H_1] + \mathbf{P}[\text{BF}_{12} < 1 \mid H_2] \mathbf{P}[H_2] + \frac{1}{2} \mathbf{P}[\text{BF}_{12} = 1] \end{aligned} \quad (2.2)$$

This can be done exactly in a surprising number of settings, as we show in the following section.

### 3. Limits of inference

Since we can compute (2.2) exactly, we are able to give exact limits of inference. For example, we can compute the minimal number of independent loci  $J$  such that the probability of identifying the true population size history function using any test is at least  $1 - \alpha$  for any  $\alpha \in (1/2, 1)$ . This section is devoted to deriving these results.

### 3.1. One coalescent time

Under prior probability of  $1/2$  assigned to each outcome, the Bayes factor is exactly the likelihood ratio, and the probability of selecting  $H_1$  is the probability that  $\text{BF}_{12} > 1$  plus half the probability that  $\text{BF}_{12} = 1$ . Further, this is the highest achievable probability of correct classification for any classifier. We do calculations directly using the likelihood ratio/Bayes factor. Define

$$\Lambda(w, x) \equiv \int_w^x \frac{1}{N_e(t)} dt.$$

For shorthand we write  $\Lambda(x) = \Lambda(0, x)$ .  $\Lambda : \mathbb{R}_+ \rightarrow \mathbb{R}_+$  is a monotone strictly increasing function, which is enough to guarantee the existence of an inverse

$$\Lambda^{-1}(t) = x \iff \Lambda(x) = t,$$

a fact we will use later. We have the following result:

**Theorem 3.1.** *Suppose  $n = 2$  in (2.1) and define*

$$\delta \equiv \frac{abN_0}{b-a} \log \frac{b}{a} = \frac{abN_0}{a-b} \log \frac{a}{b} \geq 0.$$

*Then*

$$\mathbf{P}[\vartheta(x) = \vartheta] = \frac{1}{2} + \frac{1}{2} e^{-\Lambda(T)} \left( e^{-\frac{\delta \wedge S}{(a \vee b)N_0}} - e^{-\frac{\delta \wedge S}{(a \wedge b)N_0}} \right)$$

*and the Bayes error rate is*

$$\frac{1}{2} - \frac{1}{2} e^{-\Lambda(T)} \left( e^{-\frac{\delta \wedge S}{(a \vee b)N_0}} - e^{-\frac{\delta \wedge S}{(a \wedge b)N_0}} \right).$$

*Proof.* The likelihood ratio for  $H_1$  vs  $H_2$  can be expressed by

$$\log \text{BF}_{12}(x) = \begin{cases} 0 & x < T \\ \log \frac{b}{a} - \frac{x-T}{aN_0} + \frac{x-T}{bN_0} & T \leq x < T+S \\ \frac{S}{bN_0} - \frac{S}{aN_0} & T+S \leq x \end{cases} \quad (3.1)$$

Notice that the waiting time until the coalescent event has survival function

$$\mathbf{P}[X > x] = e^{-\Lambda(x)}.$$

Now we want to calculate  $\mathbf{P}[\vartheta(x) = 1 \mid H_1]$ . Assume that if  $\log \text{BF}_{12}(x) = 0$  we select either  $H_1$  or  $H_2$  by flipping a fair coin. If  $a > b$  then

$$\log \text{BF}_{12}(x) > 0, T \leq x \leq T+S \iff x > \delta + T,$$

and if  $b > a$

$$\log \text{BF}_{12}(x) > 0, T \leq x \leq T+S \iff x < \delta + T.$$

Assuming  $a > b$  and denoting  $f_i(x)$  the density under  $H_i$  for  $i = 1, 2$ , we have

$$\begin{aligned} \mathbf{P}[\vartheta(x) = 1 \mid H_1] &= \frac{1}{2} \mathbf{P}[X < T \mid H_1] + \int_T^{T+S} \mathbf{1}\left\{x > \frac{ab}{b-a} N_0 \log \frac{b}{a} + T\right\} f_1(x) dx \\ &\quad + \mathbf{1}\{b < a\} \mathbf{P}[X > T + S \mid H_1] \\ &= \frac{1}{2} (1 - e^{-\Lambda(T)}) + \int_{T+(\delta \wedge S)}^{T+S} e^{-\Lambda(T)} \frac{1}{aN_0} e^{-\frac{x-T}{aN_0}} dx + \mathbf{1}_{\{b < a\}} e^{-\Lambda(T) - \frac{S}{aN_0}} \\ &= \frac{1}{2} (1 - e^{-\Lambda(T)}) + e^{-\Lambda(T)} \left[ e^{-\frac{\delta \wedge S}{aN_0}} - e^{-\frac{S}{aN_0}} \right] + \mathbf{1}_{\{b < a\}} e^{-\Lambda(T) - \frac{S}{aN_0}}, \end{aligned}$$

and

$$\begin{aligned} \mathbf{P}[\vartheta(x) = 2 \mid H_2] &= \frac{1}{2} \mathbf{P}[X < T \mid H_2] + \int_T^{T+S} \mathbf{1}\left\{x < \frac{ab}{b-a} N_0 \log \frac{b}{a} + T\right\} f_2(x) dx \\ &\quad + \mathbf{1}\{a < b\} \mathbf{P}[X > T + S \mid H_2] \\ &= \frac{1}{2} (1 - e^{-\Lambda(T)}) + \int_T^{T+(\delta \wedge S)} e^{-\Lambda(T)} \frac{1}{bN_0} e^{-\frac{x-T}{bN_0}} dx + \mathbf{1}_{\{a < b\}} e^{-\Lambda(T) - \frac{S}{bN_0}} \\ &= \frac{1}{2} (1 - e^{-\Lambda(T)}) + e^{-\Lambda(T)} \left[ 1 - e^{-\frac{\delta \wedge S}{bN_0}} \right] + \mathbf{1}_{\{a < b\}} e^{-\Lambda(T) - \frac{S}{bN_0}}. \end{aligned}$$

Assuming equal prior probability of  $H_1$  and  $H_2$  we get

$$\begin{aligned} \mathbf{P}[\vartheta(x) = \vartheta] &= \frac{1}{2} (1 - e^{-\Lambda(T)} + e^{-\Lambda(T) - \frac{S}{(a \vee b)N_0}}) \\ &\quad + \frac{1}{2} e^{-\Lambda(T)} \left[ e^{-\frac{\delta \wedge S}{aN_0}} - e^{-\frac{S}{aN_0}} \right] + \frac{1}{2} e^{-\Lambda(T)} \left[ 1 - e^{-\frac{\delta \wedge S}{bN_0}} \right] \\ &= \frac{1}{2} + \frac{1}{2} e^{-\Lambda(T)} \left( e^{-\frac{S}{(a \vee b)N_0}} - e^{-\frac{S}{aN_0}} \right) + \frac{1}{2} e^{-\Lambda(T)} \left( e^{-\frac{\delta \wedge S}{aN_0}} - e^{-\frac{\delta \wedge S}{bN_0}} \right) \\ &= \frac{1}{2} + \frac{1}{2} e^{-\Lambda(T)} \left( e^{-\frac{\delta \wedge S}{aN_0}} - e^{-\frac{\delta \wedge S}{bN_0}} \right). \end{aligned}$$

This assumed  $a > b$ . If instead  $b > a$  then the inequalities in the integrand when we integrate between  $T$  and  $T + S$  would be reversed, so the exact expression is

$$\mathbf{P}[\vartheta(x) = \vartheta] = \frac{1}{2} + \frac{1}{2} e^{-\Lambda(T)} \left( e^{-\frac{\delta \wedge S}{(a \vee b)N_0}} - e^{-\frac{\delta \wedge S}{(a \wedge b)N_0}} \right). \quad (3.2)$$

□

So we obtain an explicit expression for the Bayes error rate. Type I and type II error rates can be obtained from the conditional probability expressions derived in the proof of Theorem 3.1. In Figure 1, we compare our results to the Hellinger bounds of [9] for different values of  $a, b, N_0$ . The upper bound based on the Hellinger distance from [9] is given by

$$\frac{1}{2} + \frac{1}{2} \sqrt{2H^2(f_1, f_2)}$$

with  $H^2(f_1, f_2)$  as in (A.3). Evidently the Hellinger bound is quite loose when  $|a - b|$  is not near zero.

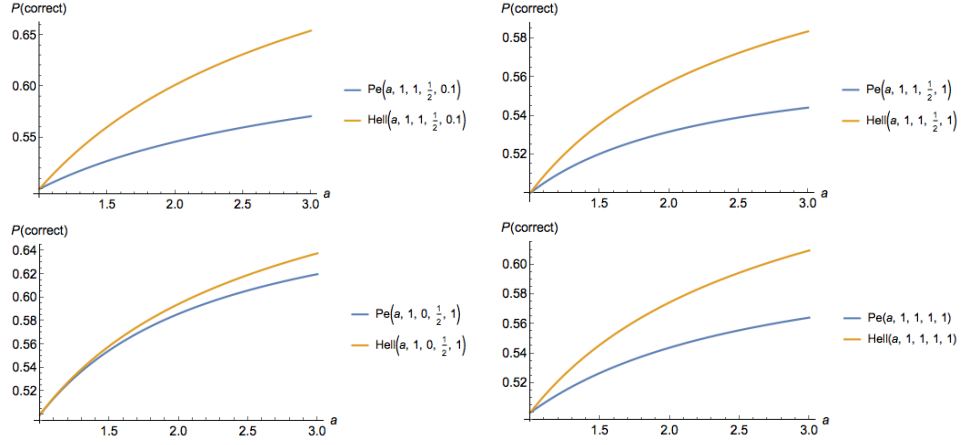


FIG 1. Exact  $\mathbf{P}[\vartheta(x) = \vartheta]$  (blue) and upper bound on this quantity from [9] (yellow) for different values of  $T, S$ , and  $N_0$ .

### 3.1.1. Extending Theorem 3.1 for $J$ loci

We now show that it is possible to obtain an exact expression for the Bayes error rate in the case of  $n = 2$  for any number of loci  $J$  in terms of the cumulative distribution function (CDF) of a sum of truncated exponentials. This function can be computed to arbitrary numerical precision.

**Theorem 3.2.** Fix an integer  $J \geq 1$  and define  $a_1 = a, a_2 = b$  for ease of notation. Let  $L = (L_1, L_2, L_3)$  have distribution conditional on the truth  $H_i$  given by

$$L \mid H_i \sim \text{Multinomial}(J, p(H_i))$$

where

$$\begin{aligned} p_1(H_i) &= \mathbf{P}[t \leq T \mid H_i] = (1 - e^{-\Lambda(T)}) \\ p_2(H_i) &= \mathbf{P}[T < t \leq T + S \mid H_i] = (e^{-\Lambda(T)} - e^{-\Lambda(T) - \frac{S}{a_i N_0}}) \\ p_3(H_i) &= \mathbf{P}[t > T + S \mid H_i] = e^{-\Lambda(T) - \frac{S}{a_i N_0}}, \end{aligned}$$

Let

$$\ell \in \{\ell = (\ell_1, \ell_2, \ell_3) : \ell_j \in \mathbb{N}, \sum_j \ell_j = J\}.$$

be an element of the support of  $\text{Multinomial}(J, p)$ . Then

$$\begin{aligned} \mathbf{P}[\vartheta(x) = \vartheta] &= \frac{1}{2} \mathbf{P}(L_2 = 0 \mid H_1) + \frac{1}{2} \sum_{(\ell_2, \ell_3): \ell_2 > 0} \mathbf{P}(L = \ell \mid H_1) \mathbf{P}[T^* > \ell_2 \delta - \ell_3 S] \\ &\quad + \frac{1}{2} \sum_{(\ell_2, \ell_3): \ell_2 > 0} \mathbf{P}(L = \ell \mid H_2) \mathbf{P}[T^* < \ell_2 \delta - \ell_3 S] \end{aligned}$$



*Proof.* We first define the following auxiliary functions

$$\begin{aligned} Q_i(T) &\equiv e^{-\int_0^T \frac{dt}{N_i(t)}}, & Q_i(T, T+S) &\equiv e^{-\int_T^{T+S} \frac{dt}{N_i(t)}} \\ q_i(T) &\equiv \frac{1}{N_i(T)} e^{-\int_0^T \frac{dt}{N_i(t)}}, & q_i(T, T+S) &\equiv \frac{1}{N_i(T+S)} e^{-\int_T^{T+S} \frac{dt}{N_i(t)}} \end{aligned}$$

The coalescent density for a coalescent time with effective population size trajectory  $N$  for the intervals  $(0, T]$  and  $(T+S, \infty)$  and  $N_i$  for the interval  $(T, T+S]$  is

$$f_i(t) = \begin{cases} q(t) & 0 < t < T \\ Q(T)q_i(T, t) & T \leq t < T+S \\ Q(T)Q_i(T, T+S)q(T+S, t) & t \geq T+S \end{cases}$$

so that the likelihood ratio for a single time point can be expressed as

$$\begin{aligned} \frac{f_1(t_j)}{f_2(t_j)} &= \left[ \frac{q_1(T, t_j)}{q_2(T, t_j)} \right]^{\mathbf{1}\{T \leq t_j < T+S\}} \left[ \frac{Q_1(T, T+S)}{Q_2(T, T+S)} \right]^{\mathbf{1}\{t_j \geq T+S\}} \\ &= \left[ \frac{b}{a} e^{-\frac{(b-a)(t_j-T)}{abN_0}} \right]^{\mathbf{1}\{T \leq t_j < T+S\}} \left[ e^{-S\frac{(b-a)}{abN_0}} \right]^{\mathbf{1}\{t_j \geq T+S\}}, \end{aligned}$$

giving

$$\begin{aligned} \log \prod_{j=1}^J \frac{f_1(t_j)}{f_2(t_j)} &= \sum_{j=1}^J \mathbf{1}\{T < t_j \leq T+S\} \left[ \log \frac{b}{a} - (t_j - T) \frac{(b-a)}{abN_0} \right] \\ &\quad - \sum_{j=1}^J \mathbf{1}\{t_j > T+S\} \frac{S(b-a)}{abN_0}. \end{aligned}$$

Defining

$$\ell_1 = \sum_{j=1}^J \mathbf{1}\{t_j \leq T\}, \quad \ell_2 = \sum_{j=1}^J \mathbf{1}\{T < t_j \leq T+S\}, \quad \ell_3 = \sum_{j=1}^J \mathbf{1}\{t_j \geq T+S\},$$

we have that  $\log \text{BF}_{12} > 0$  when

$$\begin{aligned} \sum_{j=1}^J \mathbf{1}\{T < t_j \leq T+S\} \left[ \log \frac{b}{a} - (t_j - T) \frac{(b-a)}{abN_0} \right] &> \sum_{j=1}^J \mathbf{1}\{t_j > T+S\} \frac{S(b-a)}{abN_0} \\ \ell_2 \left( \log \frac{b}{a} + T \frac{(b-a)}{abN_0} \right) - \ell_3 S \frac{(b-a)}{abN_0} &> \frac{(b-a)}{abN_0} \sum_{j: t_j \in [T, T+S]} t_j \\ \ell_2 \left( \frac{abN_0}{a-b} \log \frac{a}{b} + T \right) - \ell_3 S &< \sum_{j: t_j \in [T, T+S]} t_j, \\ \ell_2 (\delta + T) - \ell_3 S &< \sum_{j: t_j \in [T, T+S]} t_j, \end{aligned}$$

where the inequality reversed since  $(b - a)/(abN_0)$  is negative.

Now,  $\log \text{BF}_{12} = 0$  only if  $t_j < T$  for all  $j = 1, \dots, J$ . In this case, we flip a fair coin and accept  $H_1$  if it shows heads. Moreover, if  $L_2 = 0$  and  $L_3 > 0$ , then  $\log \text{BF}_{12} > 0$ . Denote by  $L = (L_1, L_2, L_3)$  the random vector whose observed entries are  $\ell = (\ell_1, \ell_2, \ell_3)$ . Notice that

$$\begin{aligned} L \mid H_i &\sim \text{Multinomial}(J, p) \\ p_1 &= \mathbf{P}[t \leq T] = (1 - e^{-\Lambda(T)}) \\ p_2 &= \mathbf{P}[T < t \leq T + S] = (e^{-\Lambda(T)} - e^{-\Lambda(T) - \frac{S}{a_i N_0}}) \\ p_3 &= \mathbf{P}[t > T + S] = e^{-\Lambda(T) - \frac{S}{a_i N_0}} \end{aligned}$$

and we have

$$\begin{aligned} \mathbf{P}[\vartheta(x) = 1 \mid H_1] &= \frac{1}{2} \mathbf{P}(L_1 = J \mid H_1) + \mathbf{P}(L_2 = 0, L_3 > 0 \mid H_1) \\ &\quad + \sum_{(\ell_2, \ell_3): \ell_2 > 0} \mathbf{P}(L = \ell \mid H_1) \mathbf{P}(\text{BF}_{12} > 0 \mid L = \ell, H_1) \end{aligned}$$

with

$$\begin{aligned} \mathbf{P}[\text{BF}_{12} > 0 \mid L = \ell, H_1] &= \mathbf{P} \left[ \sum_{j: t_j \in [T, T+S]} t_j > \ell_2(\delta + T) - \ell_3 S \mid L = \ell \right] \\ &= \mathbf{P} \left[ \sum_{j: t_j \in [T, T+S]} t_j > \ell_2(\delta + T) - \ell_3 S \mid T < t_j \leq T + S \right] \\ &= \mathbf{P} \left[ \sum_{j=1}^{\ell_2} t_j^* > \ell_2 \delta - \ell_3 S \mid t_j^* < S \right] \end{aligned}$$

for  $t_j^*$  independent exponential random variables with rate  $(aN_0)^{-1}$ . So letting  $T^*(\ell_2) = \sum_{j=1}^{\ell_2} t_j^*$ , the relevant probabilities involve the CDF of the sum of  $\ell_2$  many independent exponentials with rate  $(aN_0)^{-1}$  truncated to the interval  $[0, S]$ , and we have

$$\begin{aligned} \mathbf{P}[\vartheta(x) = 1 \mid H_1] &= \frac{1}{2} \mathbf{P}(L_1 = J \mid H_1) + \mathbf{P}(L_2 = 0, L_3 > 0 \mid H_1) \\ &\quad + \sum_{(\ell_2, \ell_3): \ell_2 > 0} \mathbf{P}(L = \ell \mid H_1) \mathbf{P}[T^* > \ell_2 \delta - \ell_3 S]. \end{aligned}$$

It follows then that since  $\mathbf{P}(L_1 = J \mid H_1) = \mathbf{P}(L_1 = J \mid H_2)$ , the Bayes error rate can be written as

$$\mathbf{P}[\vartheta(x) = \vartheta] = \frac{1}{2} \mathbf{P}(L_2 = 0 \mid H_1) \quad (3.3)$$

$$\begin{aligned}
& + \frac{1}{2} \sum_{(\ell_2, \ell_3): \ell_2 > 0} \mathbf{P}(L = \ell \mid H_1) \mathbf{P}[T^* > \ell_2 \delta - \ell_3 S] \\
& + \frac{1}{2} \sum_{(\ell_2, \ell_3): \ell_2 > 0} \mathbf{P}(L = \ell \mid H_2) \mathbf{P}[T^* < \ell_2 \delta - \ell_3 S].
\end{aligned}$$

□

Although the distribution function  $\mathbf{P}[T^* < t]$  is not available in closed form, it is approximated by Monte Carlo (Figure 2).

Kim et al. [9] use the inequality  $d_H^2(X^J, Y^J) \leq J d_H^2(X, Y)$  in combination with Theorem 2.1 to obtain lower bounds on the error rate for  $J$  independent loci. They then use these lower bounds to calculate quantities like the minimal  $S$  such that the correct hypothesis will be selected with 95 percent probability for several examples. However, in our case we have an equality, which allows us to compute exactly the value of  $S$  such that the Bayes error rate is equal to  $\epsilon$  for any  $J$ . The results on the minimal number of loci  $J$  to achieve a fixed error rate are somewhat different from the results in [9].

### 3.1.2. Expansion Out-of-Africa

We now recompute the human bottleneck example from [9]. We have  $\Lambda(T) = 2.24$ ,  $a = 0.5$ ,  $b = 0.05$ ,  $N_0 = 2.732 \times 10^4$  in units of 25 year generations. Kim et al. [9] indicate that the minimal  $J$  such that any classifier can distinguish between  $H_1$  and  $H_2$  with probability at least 0.95 is 9. For  $J = 10$  they find that  $S \geq 1.3 \times 10^5$  years is necessary to achieve probability 0.95, and for  $J = 20$  they find  $S \geq 3.6 \times 10^4$  years is necessary. Figure 2 shows the probability of correct classification as a function of  $S$  in years for different values of  $J$ . For  $S \leq 2.5 \times 10^6$ , the smallest value of  $J$  for which any classifier succeeds with probability 0.95 is 35, considerably larger than the value of 9 given by [9]. For  $S = 35$ , probability 0.95 can be achieved for  $S$  larger than about  $1.35 \times 10^5$ , which is similar to the estimate of  $1.3 \times 10^5$  produced by [9] when  $J = 10$ .

Thus far, we have not considered the effect of sampling times, and have implicitly assumed that all samples are obtained at present. A simple way to address the effect of sampling times is to recompute  $\mathbf{P}[\vartheta(x) = \vartheta]$  assuming that samples are obtained from the population at the end of the bottleneck event, which is equivalent to putting  $\Lambda(T) = 0$ . Although uncommon in the study of human populations, it is sometimes possible to obtain samples of ancient DNA, making variation in the sampling time relevant. Obtaining data from the population immediately after the end of the event of interest is in some sense the optimal strategy for statistical inference on that event, and can have an enormous positive effect on inference. This is made clear by Figure 3, which shows  $\mathbf{P}[\vartheta(x) = \vartheta]$  for  $J = 2, 3, 5, 10, 15$ . For all but  $J = 2$ ,  $\mathbf{P}[\vartheta(x) = \vartheta] \geq 0.95$  can be achieved for  $S$  greater than about  $1.15 \times 10^5$ . For  $J = 15$ , it is possible to achieve  $\mathbf{P}[\vartheta(x) = \vartheta] \geq 0.95$  with  $S$  larger than about  $1.5 \times 10^4$ .

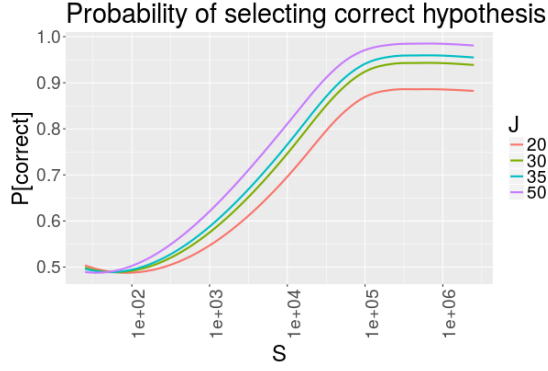


FIG 2.  $\mathbf{P}[\vartheta(x) = \vartheta]$  as a function of  $S$  for several values of  $J$  for the human bottleneck example. The function is evaluated by Monte Carlo on a grid of points and smoothed using LOESS.

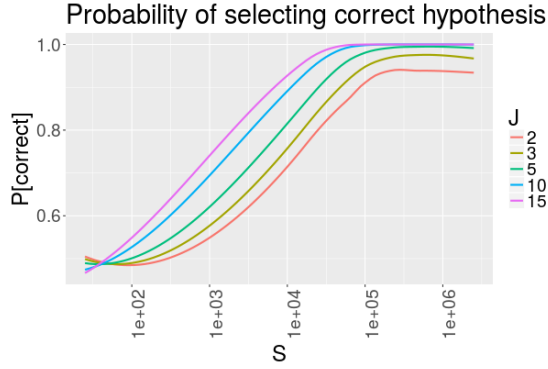


FIG 3.  $\mathbf{P}[\vartheta(x) = \vartheta]$  as a function of  $S$  for several values of  $J$  for the human bottleneck example with  $\Lambda(T) = 0$ . The function is evaluated by Monte Carlo on a grid of points and smoothed using LOESS.

### 3.2. Two coalescent times

We now consider the case of  $n = 3$  and obtain an exact expression for the probability of correct classification with  $J = 1$ . It is useful to express the likelihood as

$$L(x_2, x_1 \mid N_e(t)) = \frac{3}{N_e(x_2)N_e(x_1)} e^{-2\Lambda(x_2) - \Lambda(x_1)}.$$

**Theorem 3.3.** *For two coalescent times and a single locus, the success rate of the optimal classifier is*

$$\mathbf{P}[\vartheta(x) = \vartheta] = \frac{1}{2} + \frac{1}{4} e^{-3\Lambda(T)} \xi(a, b, N_0, T, S)$$

where

$$\begin{aligned} \xi(a, b, N_0, T, S) = & 3e^{2\Lambda(T)} \left[ e^{-\frac{\delta \wedge S}{aN_0}} - e^{-\frac{\delta \wedge S}{bN_0}} \right] \\ & + 3 \left[ e^{-\frac{2(0 \vee (\frac{\delta-S}{2} \wedge S)) + S}{aN_0}} - e^{-\frac{2(0 \vee (\frac{\delta-S}{2} \wedge S)) + S}{bN_0}} \right] - 3 \left[ e^{-\frac{\delta \wedge S}{aN_0}} - e^{-\frac{\delta \wedge S}{bN_0}} \right] \\ & + \begin{cases} 0 & S < \frac{2}{3}\delta \\ e^{-\frac{2\delta}{bN_0}} \left( 1 + \frac{2\delta-3S}{bN_0} \right) - e^{-\frac{2\delta}{aN_0}} \left( 1 + \frac{2\delta-3S}{aN_0} \right) & \frac{2}{3}\delta < S < 2\delta \\ e^{-\frac{2\delta}{aN_0}} \left( \frac{4\delta}{aN_0} + 2 \right) + e^{-\frac{2\delta}{bN_0}} - 3e^{-\frac{T-2\delta-S}{bN_0}} + e^{-\frac{2\delta+S}{bN_0}} \frac{3T-3S-4\delta}{bN_0} & S > 2\delta \end{cases} \end{aligned}$$

The proof is located in Appendix B. We can use this result to assess how much an additional sample helps in identifying the true population size history. Figure 4 shows four examples of  $\mathbf{P}[\vartheta(x) = \vartheta]$  as a function of  $a$ . In two of the examples,  $N_e(t) = 1$  outside the interval  $[T, T + S]$ , and in the other two  $N_e(t) = e^t$  outside this interval. In both cases, the probability of identifying the true effective population size function is considerably higher with  $n = 3$  than  $n = 2$  when  $|a - b|$  is not too close to zero.

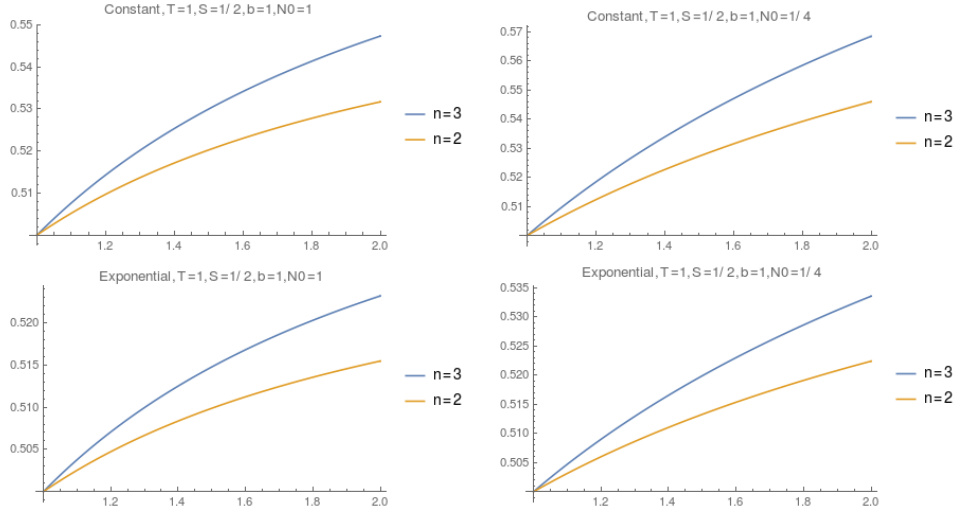


FIG 4.  $\mathbf{P}[\vartheta(x) = \vartheta]$  as a function of  $a$  for  $n = 2$  and  $n = 3$  for constant population size and exponential growth.

### 3.3. Other scenarios

In the special case where  $n = 2$ ,  $T = 0$  and  $S = \infty$  we can obtain exact results for any  $J$ . Consider the general hypothesis

$$H_1 : N_e(t) = N_1(t)$$

$$H_2 : N_e(t) = N_2(t).$$

In this case

$$\begin{aligned} \log \text{BF}_{12}(x) &= \log \frac{N_2(x)}{N_1(x)} - \int_0^x \frac{1}{N_1(t)} dt + \int_0^x \frac{1}{N_2(t)} dt \\ &= \log \frac{N_2(x)}{N_1(x)} - \Lambda_1(x) + \Lambda_2(x) \end{aligned}$$

so that with

$$\log \text{BF}_{12}(x) > 0 \Leftrightarrow \Lambda_2(x) - \Lambda_1(x) > \log \frac{N_1(x)}{N_2(x)}$$

and therefore

$$\mathbf{P}[\vartheta(x) = 1 \mid H_1] = \int_0^\infty \mathbf{1} \left\{ \Lambda_2(x) - \Lambda_1(x) > \log \frac{N_1(x)}{N_2(x)} \right\} \frac{1}{N_1(x)} e^{-\int_0^x \frac{1}{N_1(t)} dt} dx.$$

In the case where  $N_2(t) = cN_1(t)$ , we have the following result

**Theorem 3.4.** *Suppose  $N_2(t) = cN_1(t)$  and  $0 < c < 1$ . Then*

$$\mathbf{P}[\vartheta(x) = \vartheta] = \frac{1}{2} c^{\frac{c}{1-c}} + \frac{1}{2} \left( 1 - c^{\frac{1}{1-c}} \right).$$

*Proof.*

$$\begin{aligned} \mathbf{P}[\vartheta(x) = 1 \mid H_1] &= \int_0^\infty \mathbf{1} \left\{ \left( \frac{1}{c} - 1 \right) \Lambda_1(x) > \log \frac{1}{c} \right\} \frac{1}{N_1(x)} e^{-\int_0^x \frac{1}{N_1(t)} dt} dx \\ &= \mathbf{P} \left[ X_1 > \Lambda_1^{-1} \left( \frac{c}{1-c} \log \frac{1}{c} \right) \right] \\ &= e^{-\Lambda_1 \left( \Lambda_1^{-1} \left( \frac{c}{1-c} \log \frac{1}{c} \right) \right)} = e^{\frac{c \log c}{1-c}} \\ &= c^{\frac{c}{1-c}}, \end{aligned}$$

which implicitly assumed that  $c < 1$ . Similarly

$$\begin{aligned} \mathbf{P}[\vartheta(x) = 2 \mid H_2] &= \int_0^\infty \mathbf{1} \left\{ \Lambda_2(x) - \Lambda_1(x) < \log \frac{N_1(x)}{N_2(x)} \right\} \frac{1}{N_2(x)} e^{-\int_0^x \frac{1}{N_2(t)} dt} dx \\ &= \int_0^\infty \mathbf{1} \{ \Lambda_2(x)(c-1) > \log c \} \frac{1}{N_2(x)} e^{-\int_0^x \frac{1}{N_2(t)} dt} dx \\ &= \mathbf{P} \left[ X_2 < \Lambda_2^{-1} \left( \frac{1}{c-1} \log c \right) \right] = 1 - e^{-\Lambda_2 \left( \Lambda_2^{-1} \left( \frac{1}{c-1} \log c \right) \right)} \\ &= 1 - c^{\frac{1}{1-c}} \end{aligned}$$

so then

$$\mathbf{P}[\vartheta(x) = \vartheta] = \frac{1}{2} c^{\frac{c}{1-c}} + \frac{1}{2} \left( 1 - c^{\frac{1}{1-c}} \right).$$

□

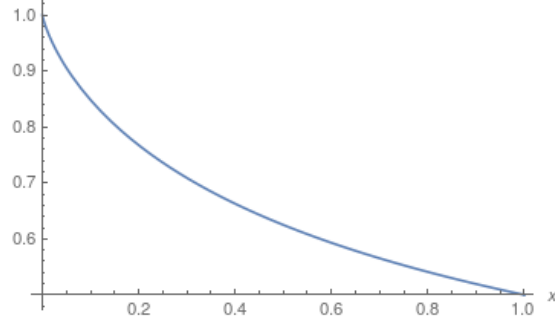
FIG 5.  $\mathbf{P}[\vartheta(x) = \vartheta]$  when  $N_2(t) = cN_1(t)$  and  $J = 1$ .

Figure 5 shows this function on the unit interval.

We can extend this calculation to  $J$  independent loci, giving the following result

**Theorem 3.5.** *Suppose  $N_2(t) = cN_1(t)$  and  $0 < c < 1$ , and  $J$  independent coalescent times are observed with  $n = 2$ . Then*

$$\begin{aligned} \mathbf{P}[\vartheta(x) = \vartheta] &= \frac{1}{2} \left( 1 - \frac{1}{\Gamma(J)} \left[ \gamma \left( J, \frac{-Jc \log c}{1-c} \right) - \gamma \left( J, \frac{J \log c}{c-1} \right) \right] \right), \quad (3.4) \\ &\equiv G(J, c). \end{aligned}$$

*Proof.* Notice that

$$\begin{aligned} \text{BF}_{12} &= \prod_{i=1}^J \frac{\frac{1}{N_1(x_i)} e^{-\int_0^{x_i} \frac{1}{N_1(t)} dt}}{\frac{1}{N_2(x_i)} e^{-\int_0^{x_i} \frac{1}{N_2(t)} dt}} = \prod_{i=1}^J \frac{N_2(x_i) e^{-\int_0^{x_i} \frac{1}{N_1(t)} dt}}{N_1(x_i) e^{-\int_0^{x_i} \frac{1}{N_2(t)} dt}} \\ &= c^J e^{-\sum_{i=1}^J \Lambda_1(x_i) - \Lambda_2(x_i)} = c^J e^{-\sum_{i=1}^J \Lambda_1(x_i) (1 - \frac{1}{c})} \\ \log \text{BF}_{12} &= J \log c - \left( 1 - \frac{1}{c} \right) \sum_{i=1}^J \Lambda_1(x_i) \end{aligned}$$

so then

$$\begin{aligned} \mathbf{P}[\log \text{BF}_{12} > 0 \mid H_1] &= \mathbf{P} \left[ J \log c > \left( 1 - \frac{1}{c} \right) \sum_{i=1}^J \Lambda_1(x_i) \mid H_1 \right] \\ &= \mathbf{P} \left[ \left( \frac{1}{c} - 1 \right) \sum_{i=1}^J \Lambda_1(x_i) > J \log \frac{1}{c} \mid H_1 \right] \\ &= \mathbf{P} \left[ \sum_{i=1}^J \Lambda_1(x_i) > J \frac{c}{1-c} \log \frac{1}{c} \mid H_1 \right]. \end{aligned}$$

Since

$$\mathbf{P}[\Lambda_1(x_i) > s \mid H_1] = \mathbf{P}[X > \Lambda_1^{-1}(s)] = e^{-s},$$

we have

$$\mathbf{P}[\log \text{BF}_{12} > 0 \mid H_1] = \mathbf{P}\left[Y > J \frac{c}{1-c} \log \frac{1}{c}\right],$$

where  $Y$  is the sum of  $J$  independent unit rate exponentials, so  $Y \sim \text{Gamma}(J, 1)$  and

$$\mathbf{P}[\log \text{BF}_{12} > 0 \mid H_1] = 1 - \frac{1}{\Gamma(J)} \gamma\left(J, J \frac{c}{1-c} \log \frac{1}{c}\right),$$

where  $\gamma(\alpha, \beta)$  is the lower incomplete Gamma function. Similar calculations give us that

$$\begin{aligned} \mathbf{P}[\log \text{BF}_{12} < 0 \mid H_2] &= \mathbf{P}\left[J \log c < (c-1) \sum_{i=1}^J \Lambda_2(x_i) \mid H_2\right] \\ &= \mathbf{P}\left[\sum_{i=1}^J \Lambda_2(x_i) < J \frac{1}{c-1} \log c \mid H_2\right] \\ &= \mathbf{P}\left[Y < J \frac{1}{c-1} \log c\right] \\ &= \frac{1}{\Gamma(J)} \gamma\left(J, J \frac{1}{c-1} \log c\right) \end{aligned}$$

giving us

$$\mathbf{P}[\vartheta(x) = \vartheta] = \frac{1}{2} \left(1 - \frac{1}{\Gamma(J)} \gamma\left(J, J \frac{c}{1-c} \log \frac{1}{c}\right) + \frac{1}{\Gamma(J)} \gamma\left(J, J \frac{1}{c-1} \log c\right)\right),$$

as claimed.  $\square$

Figure 6 shows (3.4) as a function of  $c$  for different values of  $J$ . As expected, the larger  $J$ , the larger the value of  $c$  at which high probability of identifying the true population size history can be achieved. However, even for  $J = 100$ , we must have  $c \approx 0.75$  or smaller to give probability 0.95 of selecting the true population size history. That is, the two hypotheses under consideration must be sufficiently separated.

The expression in (3.4) can be directly compared with Theorem 3.2 of [9]. Translated into our notation and conventions, this result states that

$$\mathbf{P}[\vartheta(x) = \vartheta] \leq \frac{1}{2} + \frac{1}{4} \sqrt{J(n-1)} \left(\frac{1}{c} - 1\right). \quad (3.5)$$

Figure 7 shows the bound from (3.5) along with the exact probability of identifying the true  $N_e(t)$  as a function of  $c$  for  $n = 2$  and different values of  $J$ . The bound is apparently quite loose when  $c$  is not close to 1. It becomes trivial (greater than 1) for  $c \approx 0.4$  when  $J = 1$  and  $c \approx 0.7$  when  $J = 10$ .



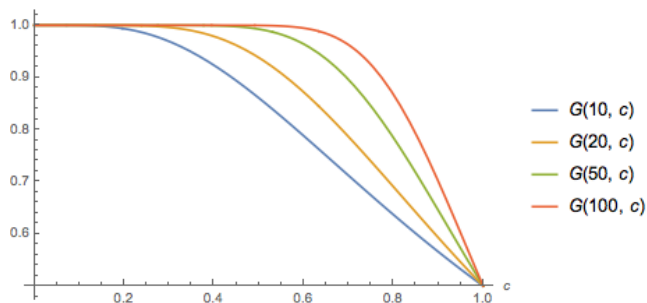
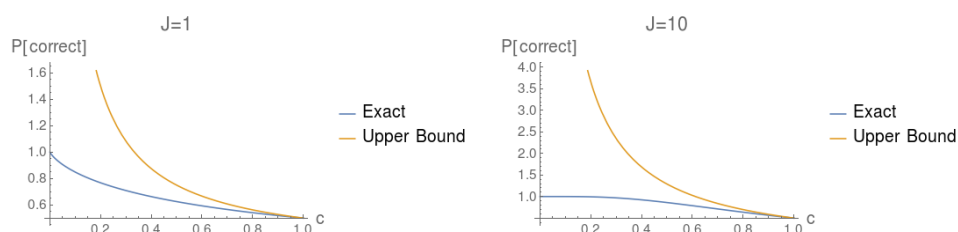


FIG 6. Several examples of the function in (3.4).

FIG 7. Exact  $\mathbf{P}[\vartheta(x) = \vartheta]$  compared to the upper bound from Theorem 3.2 of [9] as a function of  $c$  for two different values of  $J$ .

#### 4. Bayes risk under conjugate priors

Although our focus has been giving exact limits for distinguishing among two states of nature, we briefly consider estimation in the section, as the scenario in the previous section is amenable to theoretical study as an estimation problem as well. We consider the risk of estimators of the function  $\Lambda(x)$  in the case of  $n = 2$  and constant population size  $N_e(t) = \frac{1}{c}$  with conjugate priors on  $c$ . When  $n = 2$ , the coalescent time  $x$  is exponential  $c$ , so a conjugate prior is  $c \sim \text{Gamma}(\alpha, \beta)$  and for a sample of  $J$  independent loci we have

$$c \mid x^{(1)}, \dots, x^{(J)} \sim \text{Gamma}(\alpha + J, \beta + J\bar{x})$$

with expectation

$$\mathbf{E}[c \mid x^{(1)}, \dots, x^{(J)}] = \frac{\alpha + J}{\beta + J\bar{x}}.$$

Observe that

$$J\bar{X} \mid c \sim \text{Gamma}(J, c)$$

so the squared error risk of the Bayes estimator of  $c$  is

$$R(\hat{c}, c) := \int_0^\infty \left( \frac{\alpha + J}{\beta + z} - c \right)^2 \frac{\beta^\alpha}{\Gamma(\alpha)} z^{J-1} e^{-cz} dz.$$

This can be evaluated in terms of analytic functions for any  $\alpha, \beta$ , but for simplicity we focus on the simple case  $\alpha = \beta = 1$ , so that

$$\begin{aligned} R(\hat{c}, c) &= \int_0^\infty \left( \frac{1+J}{1+z} - c \right)^2 e^{-z} dz \\ &= c \left( -(J+1)e^c (J^2 + (J+3)c - 1) E_J(c) + (J+1)^2 + c \right) \end{aligned}$$

where

$$E_J(c) = \int_1^\infty \frac{e^{-cz}}{z^J} dz,$$

is a generalization of the exponential integral function. Figure 8 shows the square root of risk as a function of the number of loci  $J$  for values of  $J \in \{1, \dots, 100\}$  with  $c = 1$ . The root risk is approximately 0.1 for  $J = 100$ , and about 0.24 for  $J = 20$ . Thus, if one wants the root risk to be small relative to the truth, it is necessary to have  $J$  fairly large.

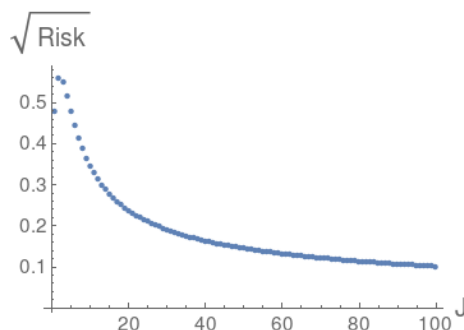


FIG 8. Root risk of Bayes estimator with  $\alpha = \beta = 1$  and  $c = 1$ .

## 5. Discussion

Assessment of statistical power in population genetic studies is becoming important in the face of ongoing large-scale studies of genetic variation. Statistical methods are usually restricted to small number of samples or rely on different approximations and non sufficient summary statistics. Many aspects of the data and model adequacy will affect our ability to draw meaningful conclusions from data. In this manuscript, we eliminate the effect of factors such as data quality, sample selection and sequence alignment and concentrate on the ideal scenario of having a complete realization of the evolutionary process free of errors. Any conclusions derived in this manuscript can be viewed as upper bounds on the achievable power of population genetic studies.

The coalescent model is the standard modeling framework for inferring evolutionary parameters from molecular sequence data. The key feature of coalescent

modeling is that it accounts for the evolutionary relationships among the samples. These evolutionary relationships are represented in a genealogy. In this manuscript, we assume that we have a realization from the coalescent process, that is, we observe a genealogy. In the multiple loci setting, we assume we have multiple independent realizations of the process. In this admittedly idealized setting, we address the key questions of which scientific hypotheses can be assessed on the basis of genealogies and the optimal choice of the number of loci, sampling times, and individuals to include in a sample to achieve a specific inferential goal. We give exact limits of inference in the binary hypothesis setting as a function of the number of loci and number of samples in realistic settings such as the expansion out-of-Africa. This work should provide some guidance to practitioners in choosing a sampling design subject to computational constraints. These results also offer a possible explanation for disagreement in the literature over timing and duration of historical genetic events such as the Out of Africa human population bottleneck, suggesting that the obtainable data may simply be insufficient to distinguish between the hypotheses of interest with high probability.

## Appendix A: Proof of Theorem 2.1

We have

$$f_i(x) = \begin{cases} \frac{1}{N_e(x)} e^{-\int_0^x \frac{1}{N_e(t)} dt} & x < T \\ \frac{1}{a_i N_0} e^{-\int_0^T \frac{1}{N_e(t)} dt} e^{-\frac{x-T}{a_i N_0}} & T \leq x < T+S \\ \frac{1}{N_e(x)} e^{-\int_0^T \frac{1}{N_e(t)} dt} e^{-\frac{S}{a_i N_0}} e^{-\int_{T+S}^x \frac{1}{N_e(t)} dt} & T+S \leq x \end{cases} \quad (\text{A.1})$$

where  $f_i(x)$  is the density of a single coalescent time under  $H_i$ . Define

$$\Delta_{12}(x) \equiv (\sqrt{f_1(x)} - \sqrt{f_2(x)})^2.$$

So now we calculate

$$\int (\sqrt{f_1(x)} - \sqrt{f_2(x)})^2 dx = \int_0^T \Delta_{12}(x) dx + \int_T^{T+S} \Delta_{12}(x) dx + \int_{T+S}^\infty \Delta_{12}(x) dx$$

clearly the first term on the right is zero so

$$\int \Delta_{12}(x) dx = \int_T^{T+S} \Delta_{12}(x) dx + \int_{T+S}^\infty \Delta_{12}(x) dx.$$

Observe

$$\begin{aligned} \int_T^{T+S} \Delta_{12}(x) dx &= \int_T^{T+S} \left( \frac{1}{\sqrt{a N_0}} e^{-\frac{1}{2} \int_0^T \frac{1}{N_e(t)} dt} e^{-\frac{1}{2} \frac{x-T}{a N_0}} - \frac{1}{\sqrt{b N_0}} e^{-\frac{1}{2} \int_0^T \frac{1}{N_e(t)} dt} e^{-\frac{1}{2} \frac{x-T}{b N_0}} \right)^2 dx \\ &= e^{-\int_0^T \frac{1}{N_e(t)} dt} \int_T^{T+S} \left( \frac{1}{\sqrt{a N_0}} e^{-\frac{1}{2} \frac{x-T}{a N_0}} - \frac{1}{\sqrt{b N_0}} e^{-\frac{1}{2} \frac{x-T}{b N_0}} \right)^2 dx \end{aligned}$$

which I just plugged in to Mathematica to avoid any algebra mistakes and got

$$e^{\int_0^T \frac{1}{N_e(t)} dt} \int_T^{T+S} \Delta_{12}(x) dx = 2 - e^{-\frac{S}{a N_0}} - e^{-\frac{S}{b N_0}} - \frac{4b(1 - e^{-\frac{(a+b)S}{2abN_0}}) \sqrt{a}}{(a+b)\sqrt{b}} \quad (\text{A.2})$$

and now

$$\begin{aligned} \int_{T+S}^\infty \Delta_{12}(x) dx &= \int_{T+S}^\infty \left( \frac{1}{\sqrt{N_e(x)}} e^{-\frac{1}{2} \int_0^T \frac{1}{N_e(t)} dt} e^{-\frac{1}{2} \frac{S}{a N_0}} e^{-\frac{1}{2} \int_{T+S}^x \frac{1}{N_e(t)} dt} \right. \\ &\quad \left. - \frac{1}{\sqrt{N_e(x)}} e^{-\frac{1}{2} \int_0^T \frac{1}{N_e(t)} dt} e^{-\frac{1}{2} \frac{S}{b N_0}} e^{-\frac{1}{2} \int_{T+S}^x \frac{1}{N_e(t)} dt} \right)^2 dx \\ &= \int \left( e^{-\frac{1}{2} \frac{S}{a N_0}} - e^{-\frac{1}{2} \frac{S}{b N_0}} \right)^2 \left( \frac{1}{\sqrt{N_e(x)}} e^{-\frac{1}{2} \int_0^T \frac{1}{N_e(t)} dt} e^{-\frac{1}{2} \int_{T+S}^x \frac{1}{N_e(t)} dt} \right)^2 dx \\ &= \left( e^{-\frac{1}{2} \frac{S}{a N_0}} - e^{-\frac{1}{2} \frac{S}{b N_0}} \right)^2 e^{-\int_0^T \frac{1}{N_e(t)} dt} \int_{T+S}^\infty \frac{1}{N_e(x)} e^{-\int_{T+S}^x \frac{1}{N_e(t)} dt} dx \end{aligned}$$

$$\begin{aligned}
&= \left( e^{-\frac{1}{2} \frac{S}{aN_0}} - e^{-\frac{1}{2} \frac{S}{bN_0}} \right)^2 e^{-\int_0^T \frac{1}{N_e(t)} dt} \left( -e^{-\int_{T+S}^x \frac{1}{N_e(t)} dt} \Big|_{T+S}^{\infty} \right) \\
&= \left( e^{-\frac{1}{2} \frac{S}{aN_0}} - e^{-\frac{1}{2} \frac{S}{bN_0}} \right)^2 e^{-\int_0^T \frac{1}{N_e(t)} dt}
\end{aligned}$$

and adding this to (A.2)

$$\begin{aligned}
H^2(f_1, f_2) &= \int \Delta_{12}(x) dx = e^{-\int_0^T \frac{1}{N_e(t)} dt} \left( 1 - e^{-\frac{(a+b)S}{2abN_0}} \right) \frac{(a+b-2\sqrt{ab})}{a+b} \\
&= e^{-\int_0^T \frac{1}{N_e(t)} dt} \left( 1 - e^{-\frac{(a+b)S}{2abN_0}} \right) \frac{(\sqrt{a}-\sqrt{b})^2}{a+b}, \quad (\text{A.3})
\end{aligned}$$

which is the same as the last displayed equation on Kim et al. [9, p 11].

## Appendix B: Proof of Theorem 3.3

Recall we are studying the case where  $H_1 : N = N_1(t)$  and  $H_2 : N = N_2(t)$  and

$$\begin{aligned}
N_1(t) &= \begin{cases} N_e(t) & 0 \leq t \leq T \\ aN_0 & T \leq t \leq T+S \\ N_e(t) & t > T+S \end{cases} \\
N_2(t) &= \begin{cases} N_e(t) & 0 \leq t \leq T \\ bN_0 & T \leq t \leq T+S \\ N_e(t) & t > T+S \end{cases}
\end{aligned}$$

for  $N_e(t)$  any bounded, strictly nonnegative function.

1. *Case 1:*  $0 < x_2 < x_1 < T$ . In this case the likelihood under either  $H_1$  or  $H_2$  is the same

$$L(x_2, x_1 \mid N_e(t)) = \frac{3}{N_e(x_2)N_e(x_1)} e^{-2\Lambda(x_2) - \Lambda(x_1)}$$

and so

$$\log \text{BF}_{12}(x) = 0.$$

2. *Case 2:*  $0 < x_2 < T < x_1 < T+S$ . In this case the likelihood under  $H_i$  is

$$L(x_2, x_1 \mid N_e(t)) = \frac{3}{N_e(x_2)} \frac{1}{a_i N_0} e^{-2\Lambda(x_2) - \Lambda(T) - \frac{x_1 - T}{a_i N_0}}$$

so designating  $a_1 = a, a_2 = b$  as before

$$\begin{aligned}
\log \text{BF}_{12}(x) &= \log \frac{b}{a} - \frac{x_1 - T}{aN_0} + \frac{x_1 - T}{bN_0} \\
&= \log \frac{b}{a} + \frac{(a-b)(x_1 - T)}{abN_0}.
\end{aligned}$$

3. *Case 3:*  $0 < x_2 < T < T + S < x_1$ . In this case the likelihood under  $H_i$  is

$$L(x_2, x_1 \mid N_e(t)) = \frac{3}{N_e(x_2)} \frac{1}{N_e(x_1)} e^{-2\Lambda(x_2) - \Lambda(T) - \frac{S}{a_i N_0} - \Lambda(T+S, x_1)}$$

so

$$\log \text{BF}_{12}(x) = \frac{S}{bN_0} - \frac{S}{aN_0} = \frac{(a-b)S}{abN_0}.$$

4. *Case 4:*  $0 < T < x_2 < x_1 < T + S$ . In this case the likelihood under  $H_i$  is

$$\begin{aligned} L(x_2, x_1 \mid N_e(t)) &= \frac{3}{a_i N_0} \frac{1}{a_i N_0} e^{-3\Lambda(T) - \frac{3(x_2-T)}{a_i N_0} - \frac{x_1-x_2}{a_i N_0}} \\ &= \frac{3}{a_i^2 N_0^2} e^{-3\Lambda(T)} e^{-\frac{2x_2+x_1-3T}{a_i N_0}} \end{aligned}$$

so

$$\begin{aligned} \log \text{BF}_{12}(x) &= 2 \log \frac{b}{a} - \frac{2x_2 + x_1 - 3T}{aN_0} + \frac{2x_2 + x_1 - 3T}{bN_0} \\ &= 2 \log \frac{b}{a} + \frac{(a-b)(2x_2 + x_1 - 3T)}{abN_0} \end{aligned}$$

5. *Case 5:*  $0 < T < x_2 < T + S < x_1$ . In this case the likelihood under  $H_i$  is

$$\begin{aligned} L(x_2, x_1 \mid N_e(t)) &= \frac{3}{a_i N_0} \frac{1}{N_e(x_1)} e^{-2\Lambda(T) - \frac{2(x_2-T)}{a_i N_0} - \Lambda(T) - \frac{S}{a_i N_0} - \Lambda(T+S, x_1)} \\ &= \frac{3}{a_i N_0} \frac{1}{N_e(x_1)} e^{-3\Lambda(T) - \Lambda(T+S, x_1)} e^{-\frac{2(x_2-T)+S}{a_i N_0}} \end{aligned}$$

so

$$\begin{aligned} \log \text{BF}_{12}(x) &= \log \frac{b}{a} - \frac{2(x_2 - T) + S}{aN_0} + \frac{2(x_2 - T) + S}{bN_0} \\ &= \log \frac{b}{a} + \frac{(a-b)(2(x_2 - T) + S)}{abN_0} \end{aligned}$$

6. *Case 6:*  $0 < T < T + S < x_2 < x_1$ . In this case the likelihood under  $H_i$  is

$$\begin{aligned} L(x_2, x_1 \mid N_e(t)) &= \frac{3}{N_e(x_2)} \frac{1}{N_e(x_1)} e^{-2\Lambda(T) - \frac{2S}{a_i N_0} - 2\Lambda(T+S, x_2) - \Lambda(T) - \frac{S}{a_i N_0} - \Lambda(T+S, x_1)} \\ &= \frac{3}{N_e(x_2)} \frac{1}{N_e(x_1)} e^{-3\Lambda(T) - 2\Lambda(T+S, x_2) - \Lambda(T+S, x_1)} e^{-\frac{3S}{a_i N_0}} \end{aligned}$$

so

$$\log \text{BF}_{12}(x) = -\frac{3S}{aN_0} + \frac{3S}{bN_0} = \frac{3(a-b)S}{abN_0}$$

$$\log \text{BF}_{12}(x) = \begin{cases} 0 & 0 < x_2 < x_1 < T \\ \log \frac{b}{a} + \frac{(a-b)(x_1-T)}{abN_0} & 0 < x_2 < T < x_1 < T+S \\ \frac{(a-b)S}{abN_0} & 0 < x_2 < T < T+S < x_1 \\ 2 \log \frac{b}{a} + \frac{(a-b)(x_1+2x_2-3T)}{abN_0} & 0 < T < x_2 < x_1 < T+S \\ \log \frac{b}{a} + \frac{(a-b)(2x_2-2T+S)}{abN_0} & 0 < T < x_2 < T+S < x_1 \\ \frac{3(a-b)S}{abN_0} & 0 < T < T+S < x_2 < x_1 \end{cases}$$

We go line by line calculating the components of  $\mathbf{P}[\text{Guess } H_1 \mid H_1]$ . Designate each of the six pieces of the expression by  $Q_j$ ,  $j = 1, 2, \dots, 6$ .

$$\begin{aligned} Q_1 &= \frac{1}{2} \mathbf{P}[X_1 < T] = \frac{1}{2} \int_0^T \int_{x_2}^T \frac{3}{N_e(x_2)N_e(x_1)} e^{-2\Lambda(x_2)-\Lambda(x_1)} \\ &= \frac{1}{2} \int_0^T (e^{-\Lambda(x_2)} - e^{-\Lambda(T)}) \frac{3}{N_e(x_2)} e^{-2\Lambda(x_2)} dx_2 \\ &= \frac{1}{2} \int_0^T \frac{3}{N_e(x_2)} e^{-3\Lambda(x_2)} dx_2 - e^{-\Lambda(T)} \int_0^T \frac{3}{N_e(x_2)} e^{-2\Lambda(x_2)} dx_2 \\ &= \frac{1}{2} \left( 1 - e^{-3\Lambda(T)} - e^{-\Lambda(T)} \frac{3}{2} \int_0^T \frac{2}{N_1(x_2)} e^{-2\Lambda(x_2)} dx_2 \right) \\ &= \frac{1}{2} \left( 1 - e^{-3\Lambda(T)} - e^{-\Lambda(T)} \frac{3}{2} (1 - e^{-2\Lambda(T)}) \right) \\ &= \frac{1}{2} + \frac{1}{4} e^{-3\Lambda(T)} - \frac{3}{4} e^{-\Lambda(T)} \end{aligned}$$

Now define

$$\delta = \frac{abN_0}{a-b} \log \frac{a}{b}$$

then we have

$$\begin{aligned} Q_2 &= \int_0^T \int_T^{T+S} \frac{3}{N_e(x_2)N_e(x_1)} e^{-2\Lambda(x_2)-\Lambda(x_1)} \mathbf{1} \left\{ \log \frac{b}{a} + \frac{(a-b)(x_1-T)}{abN_0} > 0 \right\} dx_1 dx_2 \\ &= \int_0^T \int_{T+(\delta \wedge S)}^{T+S} \frac{3}{N_e(x_2)N_e(x_1)} e^{-2\Lambda(x_2)-\Lambda(x_1)} dx_1 dx_2 \\ &= (e^{-\Lambda(T)-\frac{\delta \wedge S}{aN_0}} - e^{-\Lambda(T)-\frac{S}{aN_0}}) \frac{3}{2} \int_0^T \frac{2}{N_e(x_2)} e^{-2\Lambda(x_2)} dx_2 \\ &= (e^{-\frac{\delta \wedge S}{aN_0}} - e^{-\frac{S}{aN_0}}) e^{-\Lambda(T)} \frac{3}{2} (1 - e^{-2\Lambda(T)}) \end{aligned}$$

For case 3

$$Q_3 = \mathbf{1}\{a > b\} \int_0^T \int_{T+S}^\infty \frac{3}{N_e(x_2)N_e(x_1)} e^{-2\Lambda(x_2)-\Lambda(x_1)} dx_1 dx_2$$

$$\begin{aligned}
&= \mathbf{1}\{a > b\} e^{-\Lambda(T) - \frac{S}{aN_0}} \frac{3}{2} \int_0^T \frac{2}{N_e(x_2)} e^{-2\Lambda(x_2)} dx_2 \\
&= \frac{3}{2} \mathbf{1}\{a > b\} e^{-\Lambda(T) - \frac{S}{aN_0}} (1 - e^{-2\Lambda(T)})
\end{aligned}$$

Case 4

$$\begin{aligned}
Q_4 &= \int_T^{T+S} \int_{x_2}^{T+S} \frac{3}{N_e(x_2)N_e(x_1)} e^{-2\Lambda(x_2) - \Lambda(x_1)} \mathbf{1}\{x_1 > T + 2(T - x_2 + \delta)\} dx_1 dx_2 \\
&= \int_T^{T+S} \int_{x_2}^{T+S} \frac{3}{a^2 N_0^2} e^{-3\Lambda(T)} e^{-\frac{2x_2+x_1-3T}{aN_0}} \mathbf{1}\{x_1 > T + 2(T - x_2 + \delta)\} dx_1 dx_2.
\end{aligned}$$

The inequalities

$$0 < T < x_2 < x_1 < T + S, \quad x_1 > T + 2(T - x_2 + \delta)$$

reduce to

$$\frac{2\delta}{3} < S < 2\delta, \quad \frac{1}{3}(3T + 2\delta) < x_1 < S + T, \quad \frac{1}{2}(3T - x_1 + 2\delta) < x_2 < x_1$$

or

$$S > 2\delta$$

and either

$$\frac{1}{3}(3T + 2\delta) < x_1 < T + 2\delta, \quad \frac{1}{2}(3T - x_1 + 2\delta) < x_2 < x_1$$

or

$$T + 2\delta < x_1 < S + T, \quad T < x_2 < x_1.$$

So then we can express  $Q_4$  as

$$Q_4 = \begin{cases} 0 & S < \frac{2}{3}\delta \\ Q_{41} & \frac{2}{3}\delta < S < 2\delta \\ Q_{42} & S > 2\delta \end{cases}$$

where

$$\begin{aligned}
Q_{41} &= \int_{\frac{1}{3}(3T+2\delta)}^{T+S} \int_{\frac{1}{2}(3T-x_1+2\delta)}^{x_1} \frac{3}{a^2 N_0^2} e^{-3\Lambda(T)} e^{-\frac{2x_2+x_1-3T}{aN_0}} dx_2 dx_1 \\
&= \frac{1}{2} e^{-3\Lambda(T)} \left( e^{-\frac{3S}{aN_0}} - e^{-\frac{2\delta}{aN_0}} \frac{aN_0 - 3S + 2\delta}{aN_0} \right)
\end{aligned}$$

and

$$Q_{42} = \int_{\frac{1}{3}(3T+2\delta)}^{T+2\delta} \int_{\frac{1}{2}(3T-x_1+2\delta)}^{x_1} \frac{3}{a^2 N_0^2} e^{-3\Lambda(T)} e^{-\frac{2x_2+x_1-3T}{aN_0}} dx_2 dx_1$$



$$\begin{aligned}
& + \int_{T+2\delta}^{T+S} \int_T^{x_1} \frac{3}{a^2 N_0^2} e^{-3\Lambda(T)} e^{-\frac{2x_2+x_1-3T}{aN_0}} dx_2 dx_1 \\
& = \frac{1}{2} e^{-3\Lambda(T)} \left( e^{-\frac{6\delta}{aN_0}} + e^{-\frac{2\delta}{aN_0}} \frac{4\delta - aN_0}{aN_0} \right) \\
& + \frac{1}{2} e^{-3\Lambda(T)} \left( e^{-\frac{3S}{aN_0}} - 3e^{-\frac{S}{aN_0}} - e^{-\frac{6\delta}{aN_0}} + 3e^{-\frac{2\delta}{aN_0}} \right) \\
& = \left( \frac{1}{2} e^{-3\Lambda(T)} \left( e^{-\frac{2\delta}{aN_0}} \left( \frac{4\delta}{aN_0} + 2 \right) + e^{-\frac{3S}{aN_0}} - 3e^{-\frac{S}{aN_0}} \right) \right)
\end{aligned}$$

And now for case 5

$$\begin{aligned}
Q_5 & = \int_T^{T+S} \int_{T+S}^{\infty} f_1(x_1, x_2) \mathbf{1} \left\{ \log \frac{b}{a} + \frac{(a-b)(2(x_2-T)+S)}{abN_0} > 0 \right\} dx_1 dx_2 \\
& = \int_T^{T+S} \int_{T+S}^{\infty} \frac{3}{N_e(x_2)N_e(x_1)} e^{-2\Lambda(x_2)-\Lambda(x_1)} \mathbf{1} \left\{ x_2 > T + \frac{\delta}{2} - \frac{S}{2} \right\} dx_1 dx_2 \\
& = \int_{T+\{0 \vee ((\frac{\delta}{2}-\frac{S}{2}) \wedge S)\}}^{T+S} \frac{3}{N_e(x_2)} e^{-2\Lambda(x_2)} dx_2 \int_{T+S}^{\infty} \frac{1}{N_e(x_1)} e^{-\Lambda(x_1)} dx_1 \\
& = \frac{3}{2} e^{-\Lambda(T)-\frac{S}{aN_0}} \int_{T+\{0 \vee ((\frac{\delta}{2}-\frac{S}{2}) \wedge S)\}}^{T+S} \frac{2}{N_e(x_2)} e^{-2\Lambda(x_2)} dx_2 \\
& = \frac{3}{2} e^{-\Lambda(T)-\frac{S}{aN_0}} (e^{-2\Lambda(T+\{0 \vee ((\frac{\delta}{2}-\frac{S}{2}) \wedge S)\})} - e^{-2\Lambda(T+S)}) \\
& = \frac{3}{2} e^{-3\Lambda(T)-\frac{S}{aN_0}} (e^{-\frac{2\{0 \vee ((\frac{\delta}{2}-\frac{S}{2}) \wedge S)\}}{aN_0}} - e^{-\frac{2S}{aN_0}})
\end{aligned}$$

Finally case 6

$$\begin{aligned}
Q_6 & = \mathbf{1}\{a > b\} \int_{T+S}^{\infty} \int_{x_2}^{\infty} \frac{3}{N_e(x_2)} \frac{1}{N_e(x_1)} e^{-2\Lambda(x_2)-\Lambda(x_1)} dx_1 dx_2 \\
& = \mathbf{1}\{a > b\} \int_{T+S}^{\infty} \frac{3}{N_e(x_2)} e^{-3\Lambda(x_2)} dx_2 \\
& = \mathbf{1}\{a > b\} e^{-3\Lambda(T)-\frac{3S}{aN_0}}
\end{aligned}$$

Now we can get the other component fairly easily. We repeat the calculations conditioning on  $H_2$

$$Q_1 = \frac{1}{2} \left( 1 + \frac{1}{2} e^{-3\Lambda(T)} - \frac{3}{2} e^{-\Lambda(T)} \right)$$

case 2

$$\begin{aligned}
Q_2 & = \int_0^T \int_T^{T+S} \frac{3}{N_e(x_2)N_e(x_1)} e^{-2\Lambda(x_2)-\Lambda(x_1)} \mathbf{1} \left\{ \log \frac{b}{a} + \frac{(a-b)(x_1-T)}{abN_0} < 0 \right\} dx_1 dx_2 \\
& = \int_0^T \int_T^{T+(\delta \wedge S)} \frac{3}{N_e(x_2)N_e(x_1)} e^{-2\Lambda(x_2)-\Lambda(x_1)} dx_1 dx_2
\end{aligned}$$

$$\begin{aligned}
&= (e^{-\Lambda(T)} - e^{-\Lambda(T) - \frac{\delta \wedge S}{bN_0}}) \frac{3}{2} \int_0^T \frac{2}{N_e(x_2)} e^{-2\Lambda(x_2)} dx_2 \\
&= (1 - e^{-\frac{\delta \wedge S}{bN_0}}) e^{-\Lambda(T)} \frac{3}{2} (1 - e^{-2\Lambda(T)})
\end{aligned}$$

For case 3

$$\begin{aligned}
Q_3 &= \mathbf{1}\{b > a\} \int_0^T \int_{T+S}^\infty \frac{3}{N_e(x_2)N_e(x_1)} e^{-2\Lambda(x_2) - \Lambda(x_1)} dx_1 dx_2 \\
&= 0
\end{aligned}$$

Case 4

$$\begin{aligned}
Q_4 &= \int_T^{T+S} \int_{x_2}^{T+S} \frac{3}{N_e(x_2)N_e(x_1)} e^{-2\Lambda(x_2) - \Lambda(x_1)} \mathbf{1}\{x_1 < T + 2(T - x_2 + \delta)\} dx_1 dx_2 \\
&= \int_T^{T+S} \int_{x_2}^{T+S} \frac{3}{b^2 N_0^2} e^{-3\Lambda(T)} e^{-\frac{2x_2 + x_1 - 3T}{bN_0}} \mathbf{1}\{x_1 < T + 2(T - x_2 + \delta)\} dx_1 dx_2.
\end{aligned}$$

The inequalities

$$0 \leq T \leq x_2 \leq x_1 \leq T + S, \quad x_1 \leq T + 2(T - x_2 + \delta), \quad \delta > 0$$

reduce to

$$0 \leq S \leq \frac{2\delta}{3}, \quad T \leq x_1 \leq S + T, \quad T \leq x_2 \leq x_1, \quad \text{or}$$

$$\frac{2\delta}{3} \leq S \leq 2\delta, \quad \begin{cases} T < x_1 \leq \frac{1}{3}(3T + 2\delta), & T \leq x_2 \leq x_1 \quad \text{or} \\ \frac{1}{3}(3T + 2\delta) \leq x_1 \leq T + S & T \leq x_2 \leq \frac{1}{2}(3T - x_1 + 2\delta) \end{cases}$$

or

$$S > 2\delta, \quad \begin{cases} T < x_1 < \frac{1}{3}(3T + 2\delta), & T < x_2 < x_1 \text{ or} \\ \frac{1}{3}(3T + 2\delta) \leq x_1 \leq T + 2\delta, & T < x_2 \leq \frac{1}{2}(3T - x_1 + 2\delta) \end{cases}$$

so

$$Q_4 = \begin{cases} Q_{41} & 0 \leq S \leq \frac{2\delta}{3} \\ Q_{42} & \frac{2\delta}{3} \leq S \leq 2\delta \\ Q_{43} & S > 2\delta \end{cases},$$

where

$$\begin{aligned}
Q_{41} &= \frac{1}{2} e^{-3\Lambda(T)} \left( e^{-\frac{3S}{bN_0}} - 3e^{-\frac{S}{bN_0}} + 2 \right) \\
Q_{42} &= \frac{1}{2} e^{-3\Lambda(T)} \left( \frac{e^{-\frac{2\delta}{bN_0}} (bN_0 + 2\delta - 3S)}{bN_0} - 3e^{-\frac{S}{bN_0}} + 2 \right) \\
Q_{43} &= \frac{1}{2bN_0} e^{-3\Lambda(T)} e^{-\frac{2\delta + S}{bN_0}} \left( bN_0 \left( 2e^{\frac{2\delta + S}{bN_0}} + e^{\frac{S}{bN_0}} - 3e^{\frac{T}{bN_0}} \right) + e^{\frac{S}{bN_0}} (-4\delta - 3S + 3T) \right)
\end{aligned}$$

Case 5

$$\begin{aligned}
Q_5 &= \int_T^{T+S} \int_{T+S}^{\infty} f_1(x_1, x_2) \mathbf{1} \left\{ \log \frac{b}{a} + \frac{(a-b)(2(x_2-T)+S)}{abN_0} < 0 \right\} dx_1 dx_2 \\
&= \int_T^{T+S} \int_{T+S}^{\infty} \frac{3}{N_e(x_2)N_e(x_1)} e^{-2\Lambda(x_2)-\Lambda(x_1)} \mathbf{1} \left\{ x_2 < T + \frac{\delta}{2} - \frac{S}{2} \right\} dx_1 dx_2 \\
&= \int_T^{T+\{0 \vee ((\frac{\delta}{2}-\frac{S}{2}) \wedge S)\}} \frac{3}{N_e(x_2)} e^{-2\Lambda(x_2)} dx_2 \int_{T+S}^{\infty} \frac{1}{N_e(x_1)} e^{-\Lambda(x_1)} dx_1 \\
&= \frac{3}{2} e^{-\Lambda(T)-\frac{S}{bN_0}} \int_T^{T+\{0 \vee ((\frac{\delta}{2}-\frac{S}{2}) \wedge S)\}} \frac{2}{N_e(x_2)} e^{-2\Lambda(x_2)} dx_2 \\
&= \frac{3}{2} e^{-\Lambda(T)-\frac{S}{bN_0}} (e^{-2\Lambda(T)} - e^{-2\Lambda(T+\{0 \vee ((\frac{\delta}{2}-\frac{S}{2}) \wedge S)\})}) \\
&= \frac{3}{2} e^{-3\Lambda(T)-\frac{S}{bN_0}} (1 - e^{-\frac{2\{0 \vee ((\frac{\delta}{2}-\frac{S}{2}) \wedge S)\}}{bN_0}})
\end{aligned}$$

Case 6

$$\begin{aligned}
Q_6 &= \mathbf{1}\{b > a\} \int_{T+S}^{\infty} \int_{x_2}^{\infty} \frac{3}{N_e(x_2)} \frac{1}{N_e(x_1)} e^{-2\Lambda(x_2)-\Lambda(x_1)} dx_1 dx_2 \\
&= 0
\end{aligned}$$

## References

- [1] Peter Beerli and Joseph Felsenstein. Maximum likelihood estimation of a migration matrix and effective population sizes in  $n$  subpopulations by using a coalescent approach. *Proceedings of the National Academy of Sciences*, 98(8):4563–4568, 2001.
- [2] Joseph Felsenstein. Accuracy of coalescent likelihood estimates: Do we need more sites, more sequences, or more loci? *Molecular Biology and Evolution*, 23(3):691–700, 2006.
- [3] Joseph Felsenstein and Allen G Rodrigo. Coalescent Approaches to HIV Population Genetics. In *The Evolution of HIV*, pages 233–272. Johns Hopkins University Press, 1999. ISBN 9780801861512.
- [4] Y X Fu and W H Li. Statistical tests of neutrality of mutations. *Genetics*, 133(3):693–709, 1993.
- [5] Feng Gao and Alon Keinan. Explosive genetic evidence for explosive human population growth. *Current Opinion in Genetics and Development*, 41 (Supplement C):130 – 139, 2016. Genetics of human origin.
- [6] Lucie Gattepaille, Torsten Günther, and Mattias Jakobsson. Inferring past effective population size from distributions of coalescent times. *Genetics*, 2016. .
- [7] Robert C. Griffiths and Paul Marjoram. An ancestral recombination graph. In Peter Donnelly and Simon Tavaré, editors, *Progress in population genetics and human evolution*, volume 87 of *IMA Volumes in Mathematics and Its Applications*, pages 257–270. Springer Verlag, New York, 1997.

- [8] James C Iles, Jayna Raghwani, GL Abby Harrison, Jacques Pepin, Cyrille F Djoko, Ubald Tamoufe, Matthew LeBreton, Bradley S Schneider, Joseph N Fair, Felix M Tshala, Patrick K Kayembe, Jean Jacques Muyembe, Samuel Edidi-Basepeo, Nathan D Wolfe, Peter Simmonds, Paul Klenerman, and Oliver G Pybus. Phylogeography and epidemic history of hepatitis C virus genotype 4 in Africa. *Virology*, 464-465(100):233–243, 09 2014.
- [9] Junhyong Kim, Elchanan Mossel, Miklós Z Rácz, and Nathan Ross. Can one hear the shape of a population history? *Theoretical population biology*, 100:26–38, 2015.
- [10] John F. C. Kingman. The coalescent. *Stochastic Processes and Their Applications*, 13(3):235–248, 1982.
- [11] Heng Li and Richard Durbin. Inference of human population history from individual whole-genome sequences. *Nature*, 475(7357):493–496, July 2011.
- [12] Julia A. Palacios, John Wakeley, and Sohini Ramachandran. Bayesian non-parametric inference of population size changes from sequential genealogies. *Genetics*, 201(1):281–304, 2015.
- [13] Anna Pluzhnikov and Peter Donnelly. Optimal sequencing strategies for surveying molecular genetic diversity. 144:1247–1262, 1996.
- [14] Raazesh Sainudiin, Kevin Thornton, Jennifer Harlow, James Booth, Michael Stillman, Ruriko Yoshida, Robert Griffiths, Gil McVean, and Peter Donnelly. Experiments with the site frequency spectrum. *Bulletin of Mathematical Biology*, 73(4):829–872, 2011.
- [15] M. Slatkin and R.R. Hudson. Pairwise comparisons of mitochondrial DNA sequences in stable and exponentially growing populations. *Genetics*, 129(2):555–562, 1991.
- [16] Timothy John Sullivan. *Introduction to Uncertainty Quantification*, volume 63. Springer, 2015.
- [17] Jonathan Terhorst and Yun S. Song. Fundamental limits on the accuracy of demographic inference based on the sample frequency spectrum. *Proceedings of the National Academy of Sciences*, 112(25):7677–7682, 2015.
- [18] Yi-Gang Tong, Wei-Feng Shi, LiuDi, Jun Qian, Long Liang, Xiao-Chen Bo, Jun Liu, Hong-Guang Ren, Hang Fan, Ming Ni, Yang Sun, Yuan Jin, Yue Teng, Zhen Li, David Kargbo, Foday Dafaie, Alex Kanu, Cheng-Chao Chen, Zhi-Heng Lan, Hui Jiang, Yang Luo, Hui-Jun Lu, Xiao-Guang Zhang, Fan Yang, Yi Hu, Yu-Xi Cao, Yong-Qiang Deng, Hao-Xiang Su, Yu Sun, Wen-Sen Liu, Zhuang Wang, Cheng-Yu Wang, Zhao-Yang Bu, Zhen-Dong Guo, Liu-Bo Zhang, Wei-Min Nie, Chang-Qing Bai, Chun-Hua Sun, Xiao-Ping An, Pei-Song Xu, Xiang-Li-Lan Zhang, Yong Huang, Zhi-Qiang Mi, Dong Yu, Hong-Wu Yao, Yong Feng, Zhi-Ping Xia, Xue-Xing Zheng, Song-Tao Yang, Bing Lu, Jia-Fu Jiang, Brima Kargbo, Fu-Chu He, George F. Gao, Wu-Chun Cao, and The China Mobile Laboratory Testing Team in Sierra Leone. Genetic diversity and evolutionary dynamics of ebola virus in sierra leone. *Nature*, 524(7563):93–96, 2015.